SUPPORTING INFORMATION

1. Characterization of the SLL-1A-16 using HPLC, Mass spectrometry and MRI.

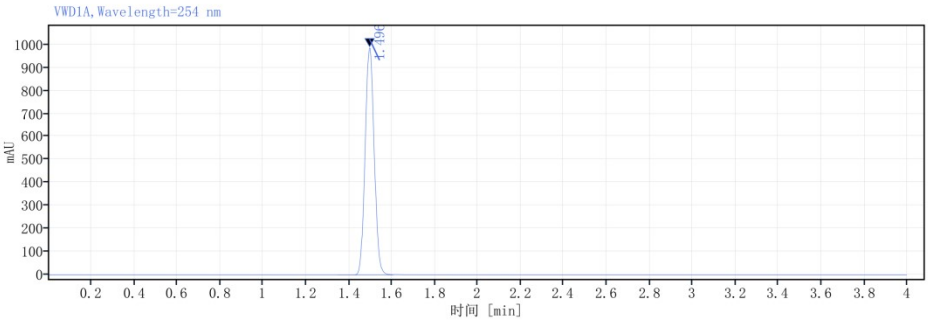

Figure S1. HPLC chromatogram of synthesized SLL-1A-16.

2.

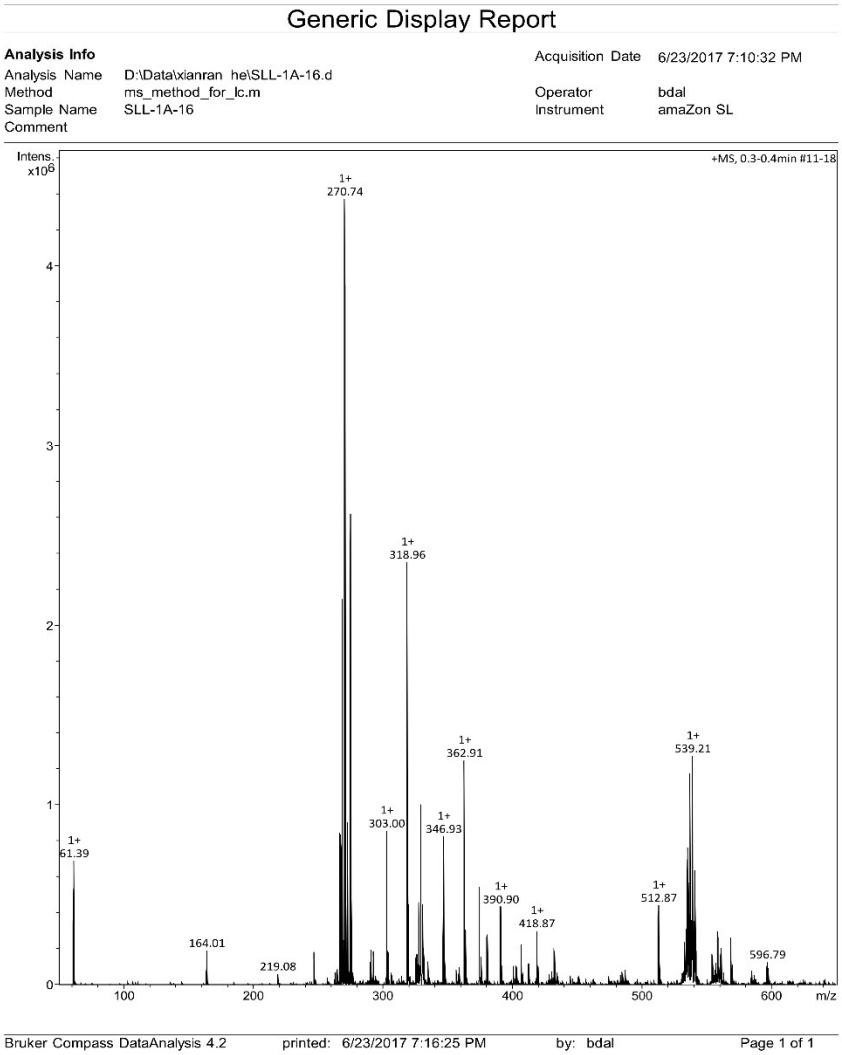

Figure S2. Mass spectrometry analysis of SLL-1A-16.

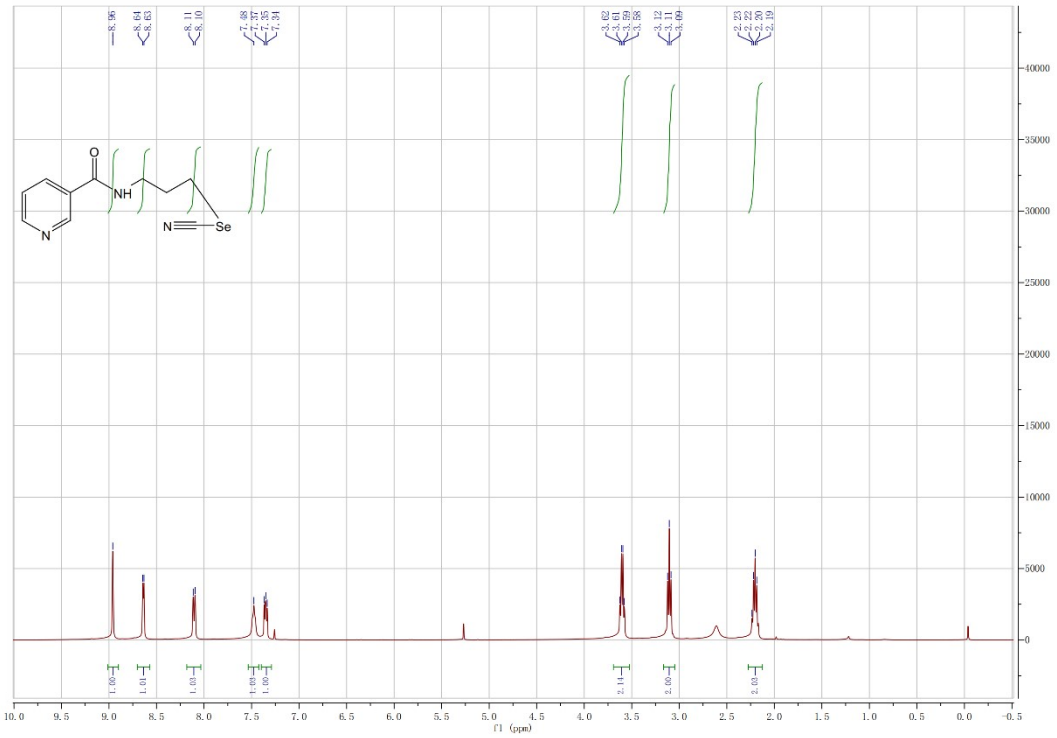

Figure S3. ^{1}H MRI analysis of SLL-1A-16.

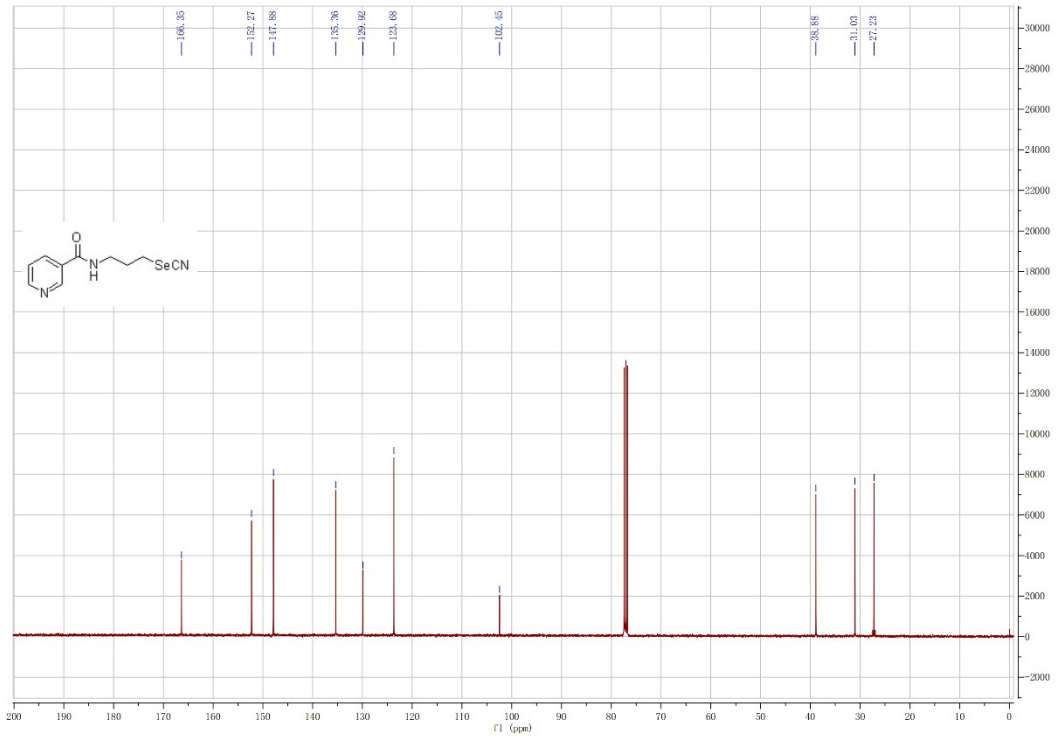

Figure S4. ^{13}C MRI analysis of SLL-1A-16.

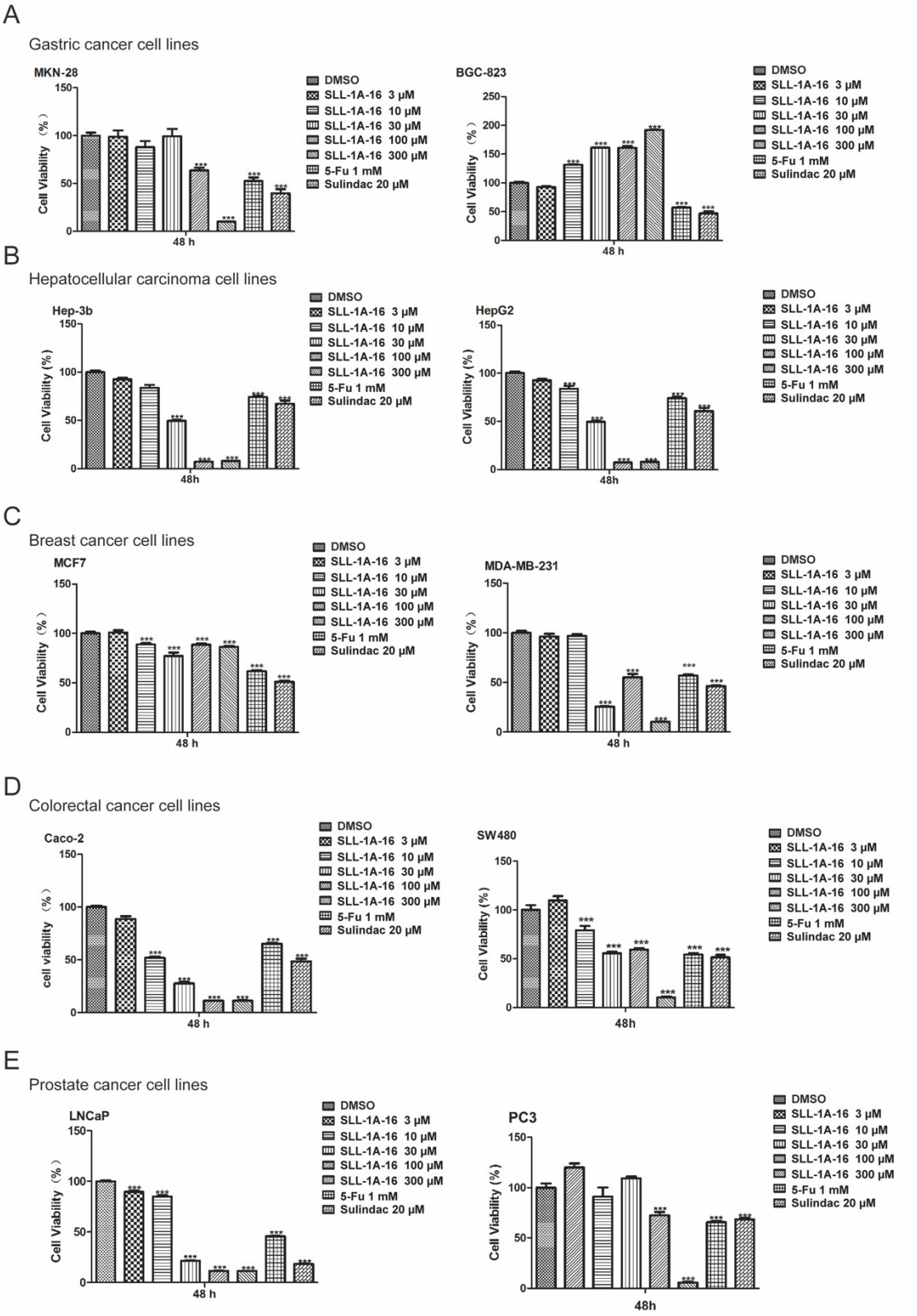

Figure S5. SLL-1A-16 inhibits proliferation of various cells. (A) The effects of SLL-1A-16 on cell viability in MKN-28 and BGC-823 cells were evaluated by CCK8 assay after treatment with increasing doses of the compound for 48 h, n=4. (B) The effects of SLL-1A-16 on cell viability in Hep-3b and HepG2 cells. (C) The effects of SLL-1A-16 on cell viability in MCF 7 and MDA-MB-221 cells. (D) The effects of SLL-1A-16 on cell viability in Caco-2 and SW480 cells. (E) The effects

of SLL-1A-16 on cell viability in LNCaP and PC3 cells. The data are presented as mean ± SD (n=4). **p < 0.01, ***p < 0.001 compared to the control group.

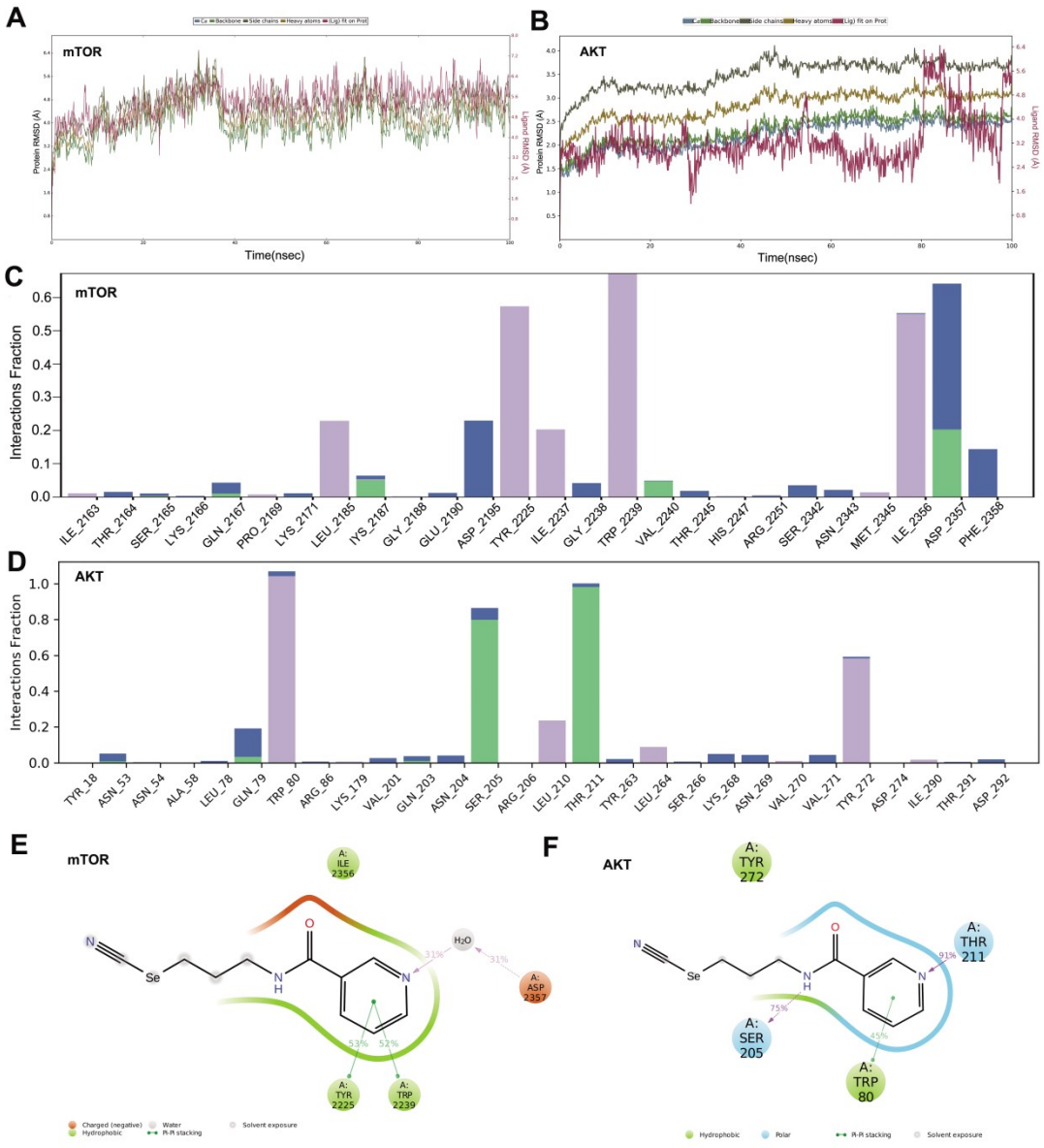

Figure S6. Molecular dynamic simulation analysis of S-400 with AKT and mTOR. (A-B) Molecular dynamics RMSD analysis of mTOR-S-400 (left) and AKT-S-400 (right) docking models over a period of 100 ns. (C-D) The protein–ligand interaction diagram of mTOR-S-400 and AKT-S-400 in MD simulations. (E) Schematic diagram of ligand interaction with the amino acid residues of protein mTOR or AKT during MD simulation.